═══════════════ **DIELECTRICS** ═══════════════

Magnetic, Electronic, and Optical Properties of the Tetraborates NiB$_4$O$_7$ and CoB$_4$O$_7$ in Three Structural Modifications

A. S. Shinkorenko[a], *, V. I. Zinenko[a], and M. S. Pavlovskii[a]

[a] *Kirensky Institute of Physics, Krasnoyarsk Scientific Center, Siberian Branch, Russian Academy of Sciences, Krasnoyarsk, 660036 Russia*

*e-mail: shas@iph.krasn.ru

Abstract—The physical properties of the NiB$_4$O$_7$ and CoB$_4$O$_7$ tetraborate compounds in three structural modifications with the sp. gr. *Pbca*, *Cmcm*, and *P*6$_5$22 have been calculated using the density functional theory in the VASP software package. The pressure dependences of the enthalpy of the compounds in the investigated structural modifications have been calculated. The calculated electron densities of states and band structures showed that the compounds under study in all the considered modifications are dielectrics with a band gap of 3−4 eV. The calculation of the magnetic exchange constants in the Heisenberg model have shown qualitative agreement with the experiment.

1. INTRODUCTION

Recently, much attention has been paid to the search for new borate compounds obtained at high pressure and temperature. The synthesis of new materials is stimulated both by the attempts to classify data on various synthesized modifications according to the growth conditions and composition and by the search for new materials with extraordinary (optical [1, 2] and magnetic [3]) properties. Such materials include the family of borates with the general chemical formula Me^{+2}B$_4$O$_7$. These compounds are implemented in the α-SrB$_4$O$_7$, α-ZnB$_4$O$_7$, and β-ZnB$_4$O$_7$ structures containing BO$_3$ triangles and/or BO$_4$ tetrahedra. As was shown experimentally [1−8], depending on the radius of the Me^{+2} ion and external conditions, the tetraborate compounds are formed in these three structural types, with rare exceptions [9].

In this study, crystals of nickel tetraborates NiB$_4$O$_7$ (NiBO) and cobalt tetraborates CoB$_4$O$_7$ (CoBO) are investigated. Both compounds exist in the phase with the sp. gr. *Cmcm* (β-NiB$_4$O$_7$ [10] and β-CoB$_4$O$_7$ [11]) with similar lattice parameters and atomic coordinates and obtained at a pressure of 7.5 GPa. In addition, a phase of cobalt tetraborate α-CoB$_4$O$_7$ with the sp. gr. *Pbca* is known [12]. The magnetic properties of this phase were studied in [13]; the antiferromagnetic ordering at a temperature of ~5 K was established. Recently [3], a new structural modification of nickel tetraborate γ-NiB$_4$O$_7$ with the sp. gr. *P*6$_5$22 was

obtained. The study of the magnetic properties of the NiB$_4$O$_7$ in the *P*6$_5$22 phase carried out in [3] showed that this compound is the so-called one-dimensional Heisenberg antiferromagnet.

The main aim of this study is to examine, using ab initio calculations, the possibility of transitions between structural modifications in the NiB$_4$O$_7$ and CoB$_4$O$_7$ compounds under hydrostatic pressure and investigate their electronic, optical, and magnetic properties in the phases with the *Pbca*, *Cmcm*, *P*6$_5$22 structures.

2. CALCULATION TECHNIQUE

The calculations were performed in the Vienna Ab initio Simulation Package (VASP) [14, 15] using the Projector Augmented Wave (PAW) pseudopotentials [16, 17]. The configuration of valence electrons is 3$d^9$4s^1 for Ni ions, 3$d^8$4s^1 for Co ions, 2$s^2$2p^1 for B ions, and 2$s^2$2p^4 ions for O ions. The functional of the exchange-correlation energy of electrons was taken into account using the generalized gradient approximation (GGA) [18]. The number of plane waves was limited to an energy of 600 eV; in the optimization of the unit cell parameters, the Monkhorst−Pack grid [19] was chosen to be 6 × 6 × 4 for the structures with the sp. gr. *Pbca*; 4 × 6 × 6 for *Cmcm*; 8 × 8 × 2 for *P*6$_5$22; and, for calculating the electronic band structure, 10 × 10 × 6 for the structures with the sp. gr. *Pbca*,
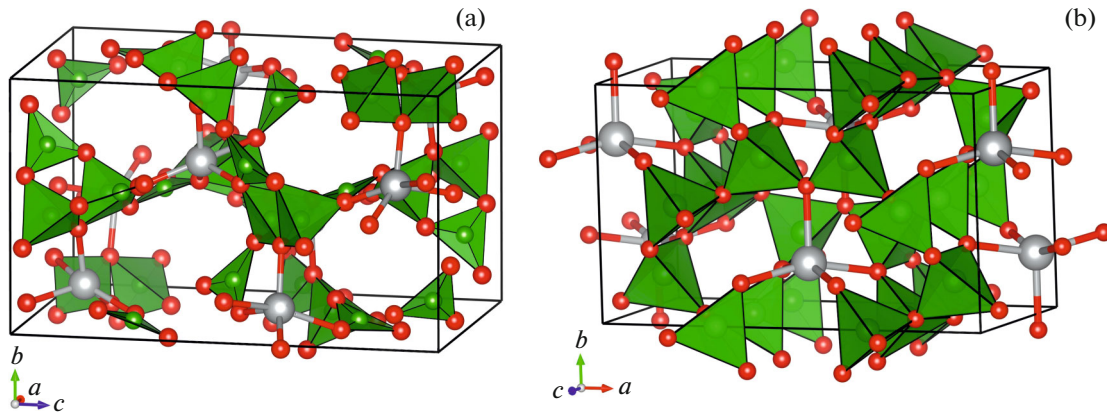
Fig. 1. Structures of the NiB_4O_7 and CoB_4O_7 tetraborate compounds with the sp. gr. (a) *Pbca* and (b) *Cmcm*.
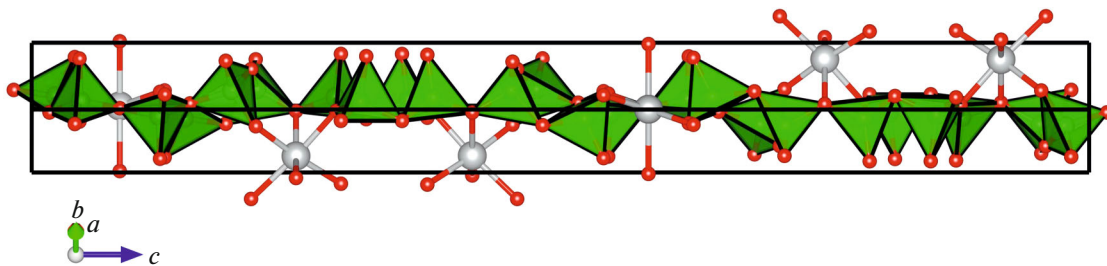
Fig. 2. Structures of the NiB_4O_7 and CoB_4O_7 tetraborate compounds with the sp. gr. $P6_522$.

$8 \times 14 \times 14$ for *Cmcm*, and $14 \times 14 \times 4$ for $P6_522$. In the calculation of the magnetic properties for enlarged cells, the Monkhorst−Pack grid was chosen to be twice as small in the corresponding direction. The strong correlations of *d* electrons of Ni and Co ions were taken into account using the GGA + U method in the Dudarev approximation [20]. The parameters and coordinates of atoms were optimized until the residual forces on the ions became weaker than 1 meV/A. In this work, the parameter *U* for Ni and Co ions is 4.5 eV. The structures of compounds were drawn in the VESTA program [21].

3. BEHAVIOR UNDER PRESSURE

The structures of the investigated compounds are shown in Figs. 1 and 2. The phase with the sp. gr. *Pbca* ($Z = 8$) consists of boron-oxygen tetrahedra and triangles forming a sparse grid with a low (~2.9 g/cm³) density [12]. The structures with the sp. gr. *Cmcm* ($Z = 4$) and $P6_522$ ($Z = 6$) consist of boron oxygen tetrahedra and are more densely packed (~3.9 g/cm³) [3].

Taking into account the similarity of Ni and Co ionic radii and the presence of an isomorphic β-phase for nickel and cobalt tetraborates with the sp. gr. *Cmcm* with similar structural parameters, we can assume that

both compounds can exist also in the above-mentioned *Pbca* and $P6_522$ phases.

To estimate the pressures at which the NiBO and CoBO compounds can exist in the *Pbca*, *Cmcm*, and $P6_522$ phases, the relaxation of cell parameters and ion coordinates at certain hydrostatic pressures was performed. In addition, the pressure dependence of the enthalpy of the polar $Pmn2_1$ phase was investigated, although this phase was not experimentally observed in the compounds under study. At each pressure, the enthalpies $H = E + PV$ (E is the total energy of the crystal, P is the pressure, and V is the cell volume) per formula unit were compared. The pressure dependences of the enthalpy for the NiBO and CoBO compounds are shown in Figs. 3 and 4, respectively; the energy of the α phase with the sp. gr. *Pbca* for the investigated compounds was taken as a reference point, since this phase has the lowest energy under normal pressure.

Let us consider the pressure dependences of the enthalpy for different phases of the NiBO compound (Fig. 3). It can be seen that, at a pressure of ~2.1 GPa, the phase with the γ-NiBO ($P6_522$) symmetry becomes energetically more favorable than the phase with the α-NiBO (*Pbca*) symmetry and, with a further increase in pressure, above 5.5 GPa, the phase with the β-NiBO symmetry (*Cmcm*) becomes more favor-
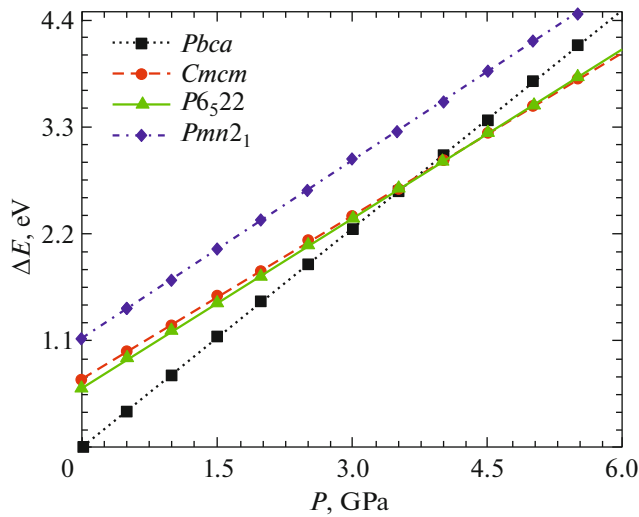
Fig. 3. Pressure dependence of the enthalpy difference between the NiB$_4$O$_7$ compounds in four structures. A reference point is the energy of the compounds with the sp. gr. *Pbca*.
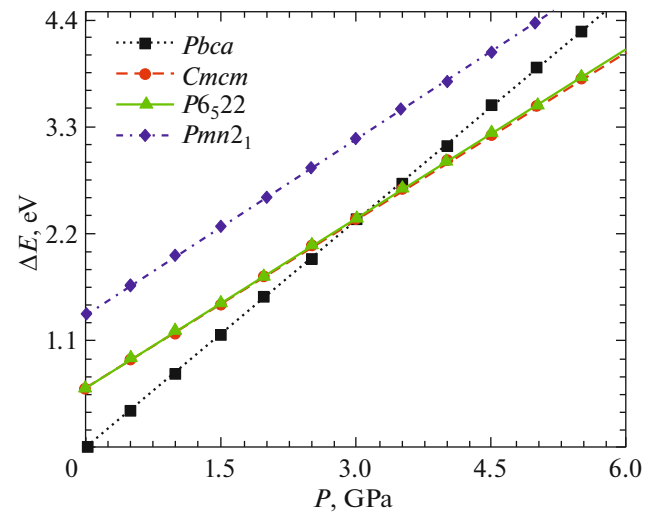
Fig. 4. Pressure dependence of the enthalpy difference between the CoB$_4$O$_7$ compounds in four structures. The reference point is the energy of the compounds with the sp. gr. *Pbca* under zero pressure.

able than both the *Pbca* and the *P*6$_5$22 phase. These results do not contradict the experimental data [3], according to which NiBO is not synthesized under normal pressure, the phase with the γ-NiBO structure (*P*6$_5$22) is obtained at a pressure of 5 GPa, and the phase with the β-NiBO structure (*Cmcm*), at a pressure of 7.5 GPa.

Let us now consider the obtained dependences of the enthalpy for different phases of the CoBO compound (Fig. 4). At zero pressure, the *Pbca* phase is energetically more favorable, while the phases of the γ-CoB$_4$O$_7$ (*P*6$_5$22) and β-CoB$_4$O$_7$ (*Cmcm*) types have similar enthalpies (the *P*6$_5$22 phase is more favorable by 0.01 eV). In the vicinity of ~3.1 GPa, the enthalpy dependence curves of the three phases intersect and, then, the β-CoB$_4$O$_7$ phase becomes most favorable. However, the enthalpy difference between the γ-CoBO (*P*6$_5$22) and β-CoBO (*Cmcm*) phases in the range from 3 to 5 GPa is insignificant, which may be indicative of the coexistence of these two phases in this pressure range. In addition, it is worth noting that the β-CoB$_4$O$_7$ synthesis occurred at a pressure of 7.5 GPa [11].

In the investigated compounds, the enthalpy of the phase with the *Pmn*2$_1$ structure is energetically extremely unfavorable (the energy difference is ~1 eV) at all the applied pressures.

4. ELECTRONIC PROPERTIES

For all the investigated structures of the NiBO and CoBO compounds, the electronic band structure and the electron densities of states were calculated. The calculated total densities of states (TDOS) and partial

densities of states (PDOS) of electrons for the NiBO and CoBO compounds of different structural types are not qualitatively different. Due to the minor differences between the electronic states of the compounds under study in three structures, Fig. 5 shows the calculated electronic band structures; Fig. 6, the electron densities of states in the NiBO and CoBO compounds in the phase with the sp. gr. *Cmcm*; and Fig. 7, the TDOS for other structures. All the TDOS and PDOS are normalized to formula unit. The band gaps Δ*E* for different structures of the compounds are given in Table 1.

The calculated TDOS and PDOS of electrons for the NiBO and CoBO compounds of different structural types are not qualitatively different. The valence band structure is nearly identical for all the structural modifications of the investigated compounds. It consists of the *d* states of Ni and Co atoms (the band center is in the range of −4...−1 eV), the *s* and *p* states of B atoms (the center and bottom of the band are between −10...−4 eV), and the *p* states of O atoms (the center and top of the band).

Small differences in the electronic structure of different phases of the compounds under study are

Table 1. Calculated band gaps Δ*E* and Δ*E*$_1$ of the NiB$_4$O$_7$ and CoB$_4$O$_7$ compounds in different structures

Parameter	NiB$_4$O$_7$			CoB$_4$O$_7$		
	*P*6$_5$22	*Cmcm*	*Pbca*	*P*6$_5$22	*Cmcm*	*Pbca*
Δ*E*, eV	3.1	2.9	3.2	3.8	3.9	3.9
Δ*E*$_1$, eV	2.7	2.5	2.0	1.4	1.5	1.0
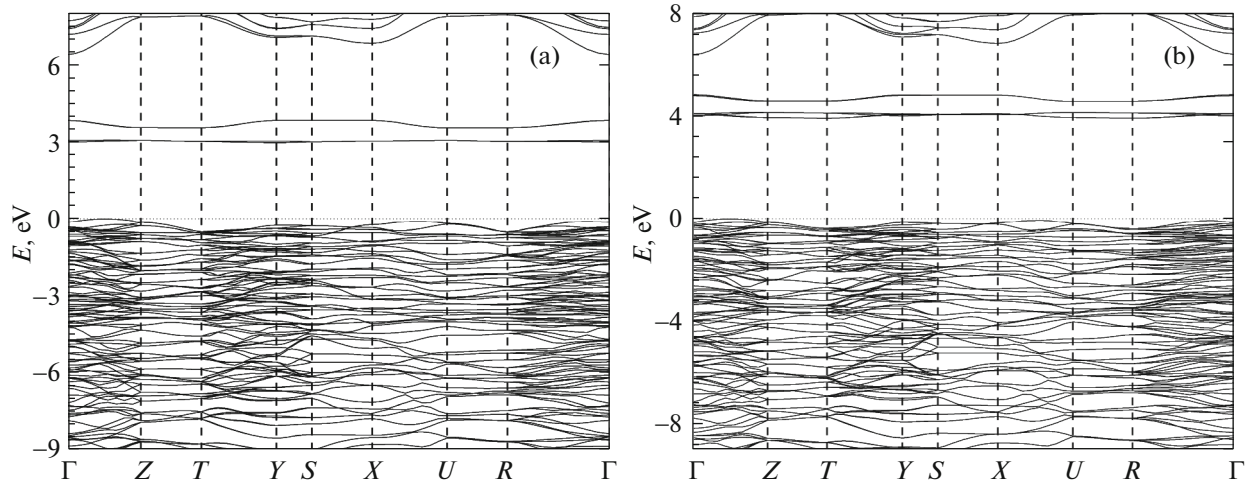
Fig. 5. Calculated electron band structures of (a) the NiB_4O_7 and (b) CoB_4O_7 compounds in the structure with the sp. gr. *Cmcm*.
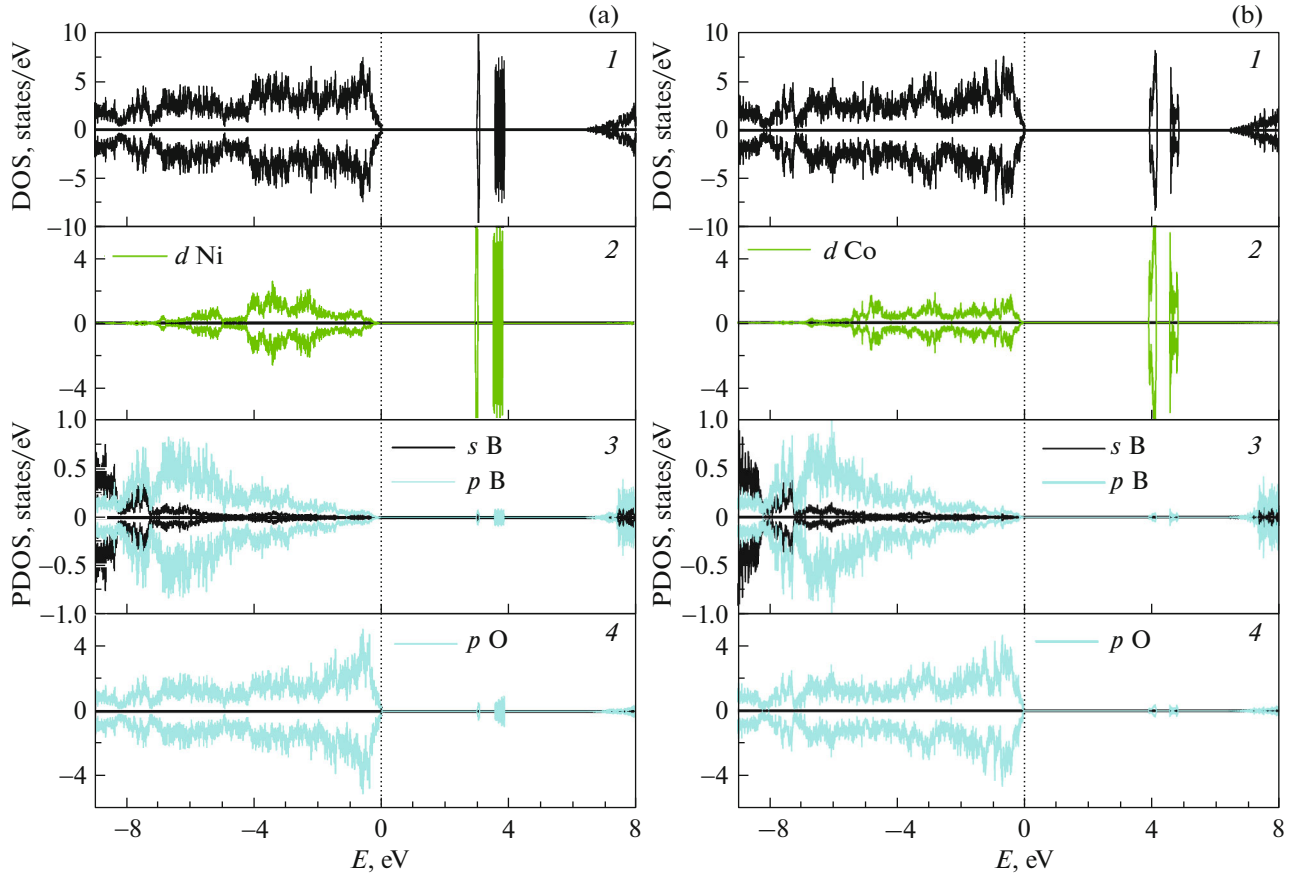
Fig. 6. Calculated (*1*) total and partial densities of states of electrons for (*2*) Ni and Co metal atoms, (*3*) B atoms, and (*4*) O atoms in (a) the NiB_4O_7 and (b) CoB_4O_7 compounds in the structure with the sp. gr. *Cmcm*.

observed in the conduction band. In all the investigated cases, the narrow lower part of the conduction band is separated from the main part (this ΔE_1 energy intervals are given in Table 1). This lower part of the conduction band consists of the *d* states of electrons of metal atoms. Depending on structure and composi-
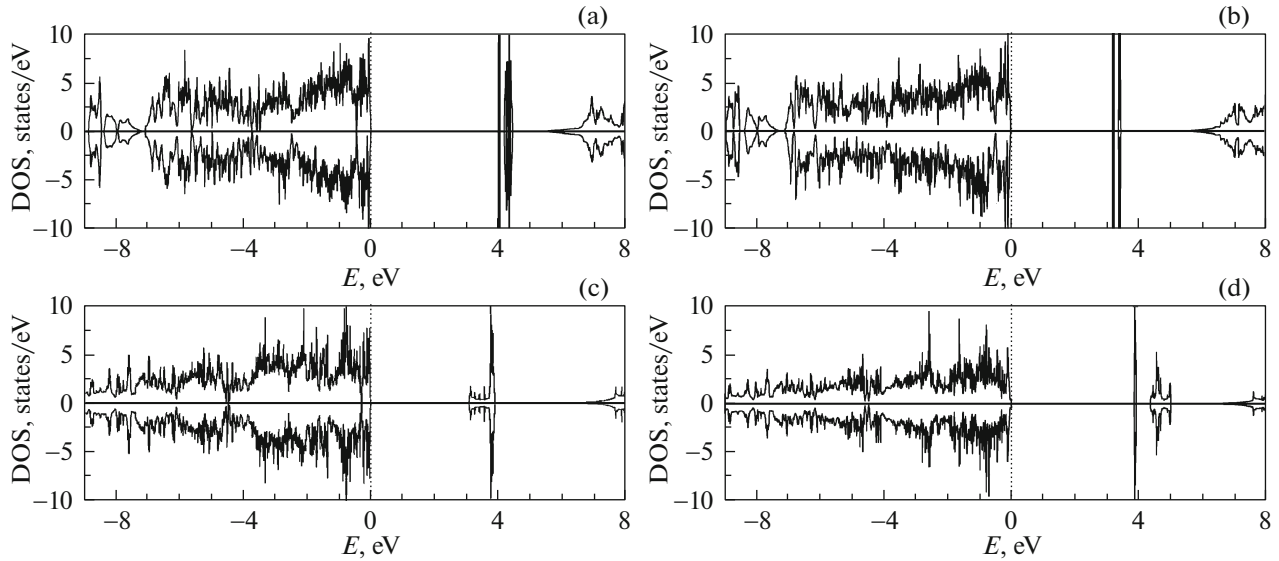
Fig. 7. Calculated electron densities of states for (a, c) the NiB_4O_7 and (b, d) CoB_4O_7 compounds in the structure with the sp. gr. *Pbca* and $P6_522$.

tion, the bottom of the conduction band changes its position relative to the upper part of the valence band, which, in turn, changes the band gap. The widest band gap is observed in the structure with the sp. gr. *Pbca* and the narrowest one, in the *Cmcm* structure (Table 1). The upper part of the conduction band for all the structures and compounds consists of the *p* states of electrons of the B atom.

5. OPTICAL PROPERTIES

For nickel and cobalt tetraborates, the frequency dependence of the dielectric function was calculated [22]. The frequency dependence of the absorptance α was calculated from the formula

$$\alpha(\omega) = \frac{2\omega}{c} \sqrt{\frac{|\varepsilon(\omega)| - \varepsilon'(\omega)}{2}}, \quad (1)$$

where $\varepsilon(\omega)$ is the complex permittivity and $\varepsilon'(\omega)$ is the real part of the permittivity. Figure 8 shows the average calculated value of the wavelength dependence of the absorptance, since no strong anisotropy was found in these compounds.

Using the obtained dependences, one can determine the absorption edge of the material, which was found to be ~400 nm in nickel tetraborate and ~320 nm in cobalt tetraborate. This is due to the narrower band gap in nickel tetraborate and, since the difference in the band gap between the structures is not large, the absorption edge in these compounds differs insignificantly. No experimental data on the optical absorption of the compounds under study were found in the literature.

6. MAGNETIC PROPERTIES

Divalent nickel and cobalt ions are magnetic and have spins $s = 1$ and $s = 3/2$, respectively. To determine the ground magnetic state and the parameters of the exchange interaction in the NiBO and CoBO crystals, we calculated the total energies for each structural modification of the crystals under study taking into account the spin polarization with different types of magnetic ordering. The exchange interaction constants were estimated in the framework of the classical Heisenberg model

$$H = -\frac{1}{2} \sum_{i,j} J_{ij} \hat{S}_i \hat{S}_j. \quad (2)$$

In the structure with the sp. gr. *Pbca*, the unit cell contains eight magnetic atoms, which form zigzag chains along the *a* direction (Fig. 9). Here, each magnetic ion has two nearest neighboring magnetic ions in the chain (exchange constant J_1) and one in the neighboring chain (exchange constant J_2). The discussed magnetic structures are shown in Fig. 9.

In the structure with the sp. gr. *Cmcm*, the unit cell contains four magnetic atoms. To describe the magnetic configurations, the cell was doubled along the *c* axis. In this structure, magnetic atoms form layers in the (*bc*) plane (Fig. 10). Each magnetic ion has six nearest magnetic ions, which form a distorted hexagon: the interaction with four neighbors with the constant J_1 and with two neighbors with the constant J_2. The distance between the layers of magnetic atoms is fairly large; therefore, the exchange interaction between atoms in neighboring layers was ignored. The investigated magnetic structures are shown in Fig. 10.
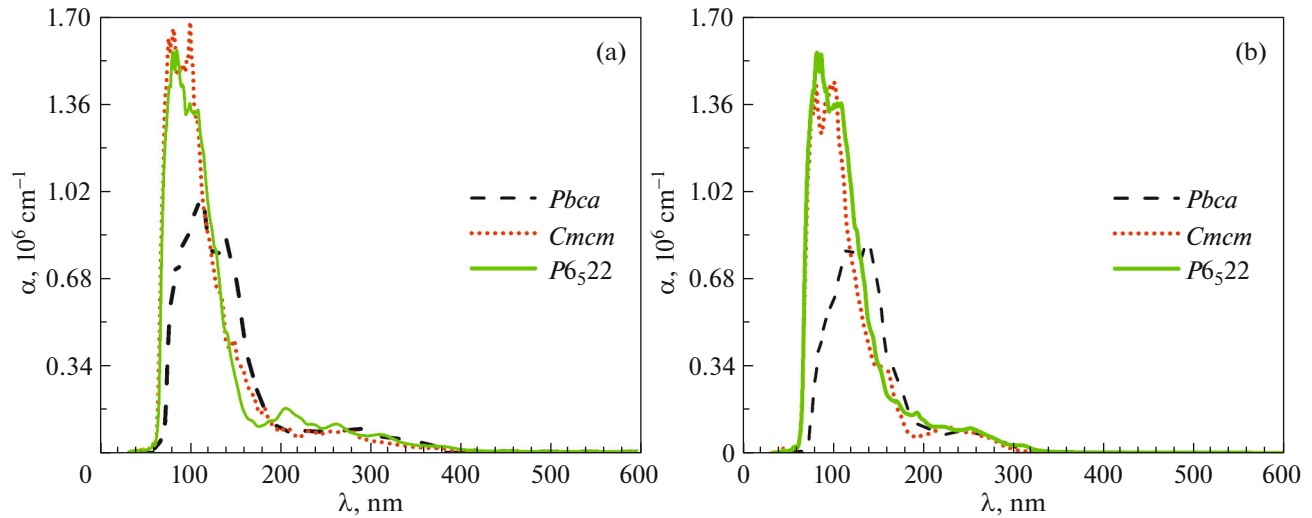
Fig. 8. Calculated dependence of the absorptance α on the wavelength for (a) the NiB_4O_7 and (b) CoB_4O_7 compounds in different structures.
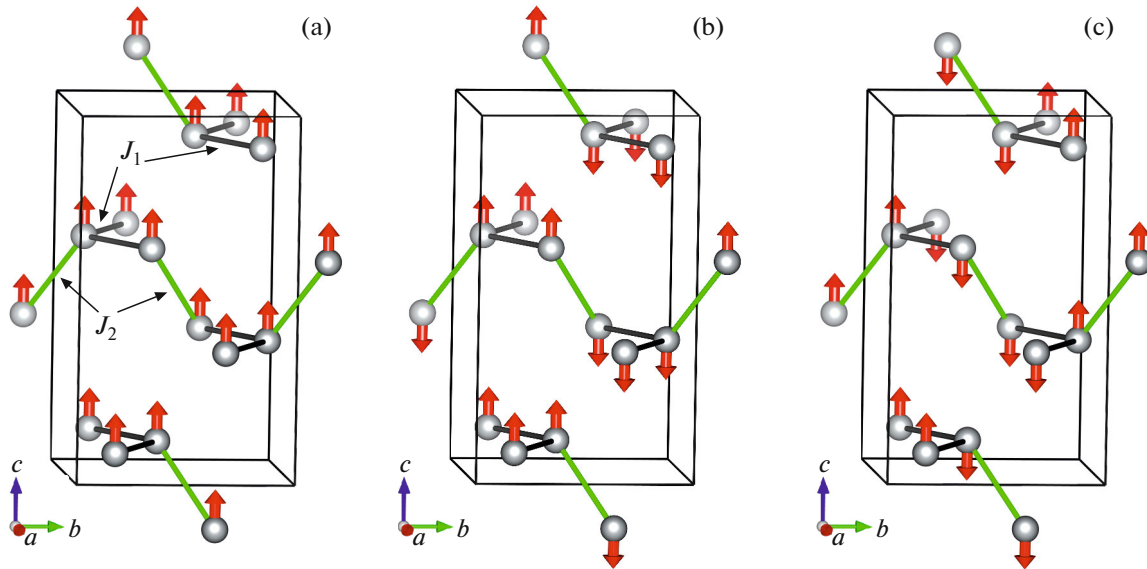
Fig. 9. Configurations of the magnetic moments in the structure with sp. gr. *Pbca*: (a) *F*, (b) AF_1, and (c) AF_2.

In the structure with the sp. gr. $P6_522$, the unit cell contains six magnetic atoms. To examine the magnetic configurations, the cell was quadrupled via doubling the *a* and *b* axes. In this structure, magnetic atoms form planes perpendicular to the *c* axis. Each magnetic atom in the plane has six nearest magnetic ions forming a regular hexagon (Fig. 11). The distance between the layers of magnetic atoms is fairly large; therefore, the exchange interaction between atoms in neighboring layers was ignored.

Although each magnetic atom has six equidistant nearest neighbors, it is necessary to use two different exchange constants. The nickel or cobalt ion in this structural type is surrounded by six oxygen ions forming an octahedron. Such oxygen octahedra sharing their vertices form infinite parallel chains in the plane perpendicular to the *c* axis (Fig. 11). Thus, the exchange constant J_1 denotes the interaction of a magnetic ion with two nearest neighbors in the chain of oxygen octahedra and the exchange constant J_2, the interaction of a magnetic ion with four nearest magnetic ions in neighboring chains.

The expressions of the energies of the investigated magnetic configurations though Hamiltonian exchange constants (1) and the calculated energies of
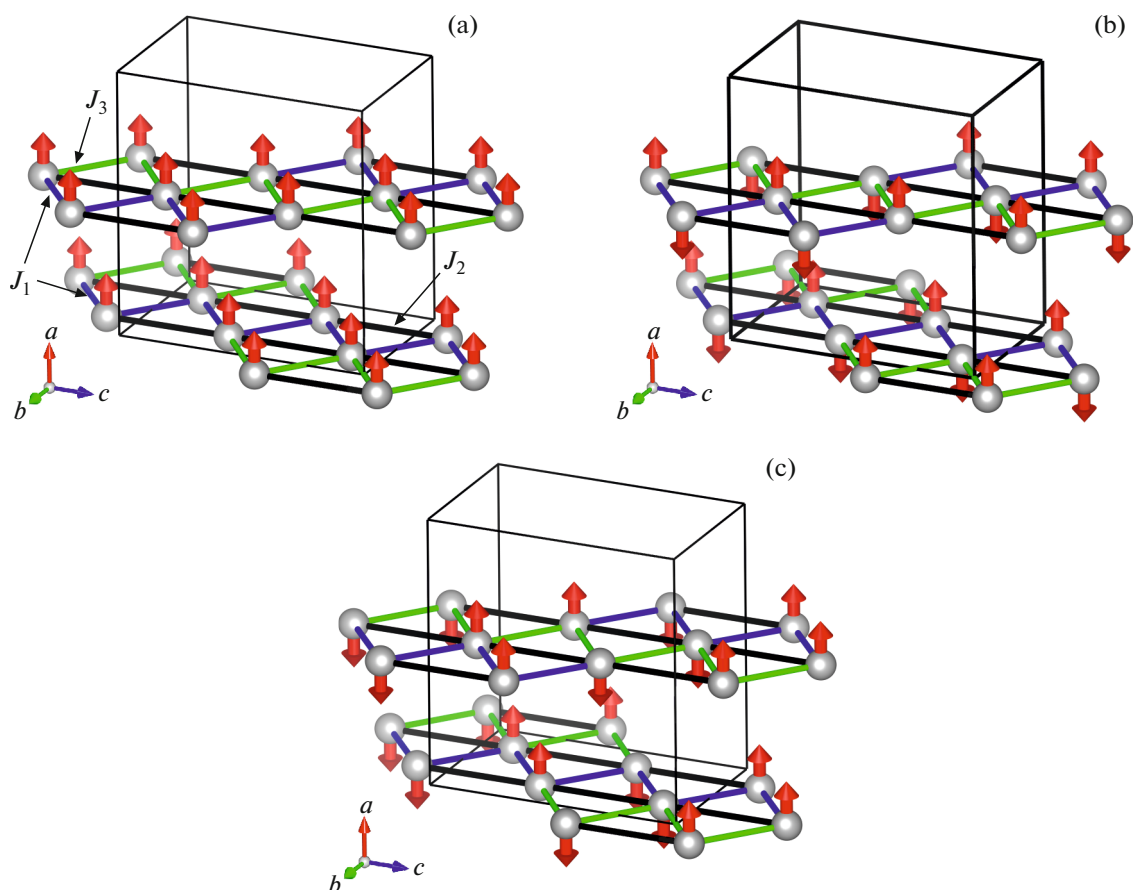
Fig. 10. Configurations of the magnetic moments in the structure with the sp. gr. *Cmcm*: (a) *F*, (b) AF_1, and (c) AF_2.
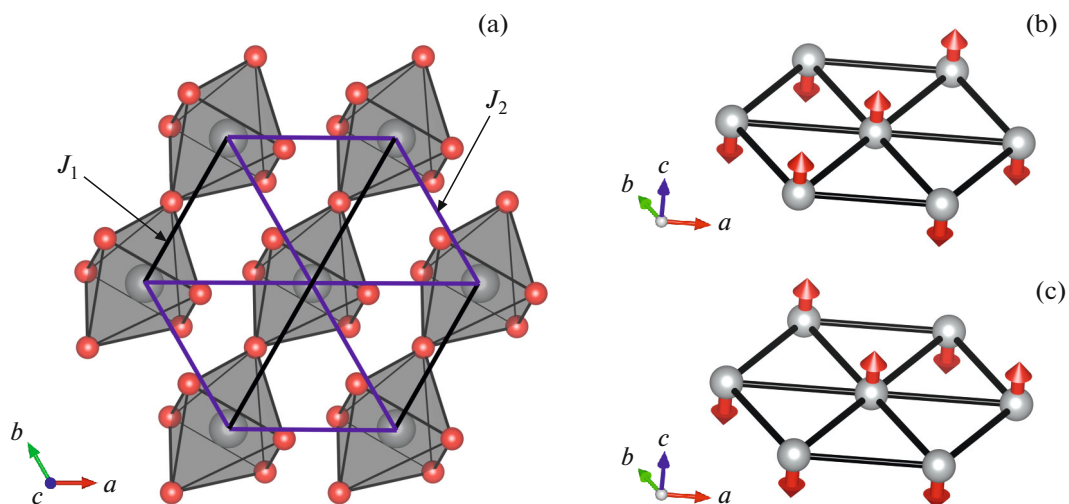
Fig. 11. (a) Chains of octahedra and configurations of the magnetic moments in the structure with the sp. gr. $P6_522$: (b) AF_1 and (c) AF_2.

these configurations relative to the energy of the ferromagnetic state for the three structural types of the NiBO and CoBO crystals are given in Table 2. The obtained exchange interaction constants are given in Table 3.

In [12], the value of the magnetic exchange for cobalt tetraborate in the *Pbca* phase was estimated from the experimental data (one constant of the exchange interaction with three nearest neighbors was taken into account), which was $J = -(0.18-0.20)$ meV.

Table 2. Calculated energies of the magnetic configurations in different structures

Configuration	Expression	NiB_4O_7	CoB_4O_7
Pbca		ΔE, meV	
F	$2J_1 + J_2$	0	0
AF_1	$2J_1 - J_2$	−1.2	−1.7
AF_2	$-2J_1 + J_2$	−0.6	−1.0
Cmcm		ΔE, meV	
F	$4J_1 + 2J_2$	0	0
AF_1	$-4J_1 + 2J_2$	−0.2	−1.9
AF_2	$-2J_1$	−0.2	−2.4
$P6_522$		ΔE, meV	
F	$2J_1 + 4J_2$	0	0
AF_1	$2J_1 - 4J_2$	0.1	0.1
AF_2	$-2J_1$	−10.1	−5.5

Table 3. Calculated energies of the magnetic configurations in different structures

Parameter	NiB_4O_7		CoB_4O_7	
	J_1, meV	J_2, meV	J_1, meV	J_2, meV
Pbca	−0.3	−1.2	−0.2	−0.7
Cmcm	−0.06	−1.21	0.09	−0.5
$P6_522$	−5.1	0.03	−2.5	0.04

In this study, the calculated exchange interaction constants for cobalt tetraborate in the *Pbca* phase were $J_1 = -0.2$ meV for two neighbors at a distance of 4.94 Å and $J_2 = -0.7$ meV with one neighbor at a distance of 4.39 Å. Thus, we can say that the resulting average value of the exchange interaction, which was found to be 0.37 meV, is in satisfactory agreement with the experimental value from [12].

In [3], a model for describing the magnetic properties of the γ-NiB_4O_7 compound was built on the basis of the experimental data, which was used to establish the one-dimensional character of the exchange interaction of magnetic moments along the chain of NiO_6 octahedra (Fig. 11a), which is consistent with the results of the calculation made in this work. Specifically, it was found that the value of the exchange interaction in the chain is greater than the value of the exchange interaction between the chains by two orders of magnitude (Table 3). As was noted in [13], the one-dimensional character of the exchange interaction is related to the following feature of this crystal structure: the Ni−O−Ni superexchange can only occur along the chain of octahedra, while in other directions there are no such bonds.

7. CONCLUSIONS

The main results obtained in this study were as follows. The pressure dependences of the enthalpy for the NiB_4O_7 and CoB_4O_7 compounds in the structures with the sp. gr. *Pbca*, *Cmcm*, and $P6_522$ were calculated. It was shown that, in the cobalt tetraborate compound, the energies of the β-CoB_4O_7 (*Cmcm*) and γ-CoB_4O_7 ($P6_522$) phases in the pressure range from 3 to 5 GPa are similar, which may be indicative of the coexistence of these phases in this pressure range. In nickel tetraborate, with increasing pressure, first the γ-NiB_4O_7 ($P6_522$) phase and, then, the β-NiB_4O_7 (*Cmcm*) phase become favorable, which is consistent with the experiments [3, 10]. In addition, the electronic band structure and the electron density of states for the NiB_4O_7 and CoB_4O_7 compounds in the investigated structures were calculated. The calculated band gaps are given in Table 1. The wavelength dependence of the absorptance was calculated and the absorption edges of the material determined from it were found to be ~400 nm for nickel tetraborate and ~320 nm for cobalt tetraborate.

The calculation of the magnetic properties of the NiB_4O_7 and CoB_4O_7 compounds showed that the ground states in different structural modifications are the states with the antiferromagnetic spin ordering. The magnetic exchange interaction constants were calculated in the framework of the classical Heisenberg model (Table 3). In the cobalt tetraborate compound, in the phase with the sp. gr. *Pbca*, the obtained exchange constants agree with those obtained in [12]. For the γ-NiB_4O_7 compound with the sp. gr. $P6_522$, the calculation, as the experiment from [3], revealed a one-dimensional character of the spin interaction.

CONFLICT OF INTEREST

The authors declare that they have no conflicts of interest.

REFERENCES

1. Yu. S. Oseledchik, A. L. Prosvirnin, A. I. Pisarevskiy, V. V. Starshenko, V. V. Osadchuk, S. P. Belokrys, N. V. Svitanko, A. S. Korol, S. A. Krikunov, and A. F. Selevich, Opt. Mater. **4**, 669 (1995).

2. A. I. Zaitsev, A. S. Aleksandrovskii, A. V. Zamkov, and A. M. Sysoev, Inorg. Mater. **42**, 1360 (2006).

3. M. K. Schmitt, O. Janka, O. Niehaus, T. Dresselhaus, R. Pöttgen, F. Pielnhofer, R. Weihrich, M. Krzhizhanovskaya, S. Filatov, R. Bubnova, L. Bayarjargal, B. Winkler, R. Glaum, and H. Huppertz, Inorg. Chem. **56**, 4217 (2017).

4. B. Winkler, A. G. Castellanos Guzman, L. Wiehl, L. Bayarjargal, and V. Milman, Solid State Sci. **14**, 1080 (2012).

5. M. Weil, Acta Crystallogr., E **59**, 40 (2003).

6. J. Krogh-Moe, Acta Chem. Scand. **18**, 2055 (1964).

7. K. Machida, H. Hata, K. Okuno, G. Adachi, and J. Shiokawa, J. Inorg. Nucl. Chem. **41**, 1425 (1979).

8. H. Emme, M. Weil, and H. Huppertz, Z. Naturforsch. **60b**, 815 (2005).

9. H. Huppertz, Z. Naturforsch. **58b**, 257 (2003).

10. J. S. Knyrim, J. Friedrichs, S. Neumair, F. Roeßner, Y. Floredo, S. Jakob, D. Johrendt, R. Glaum, and H. Huppertz, Solid State Sci. **10**, 168 (2008).

11. S. C. Neumair, J. S. Knyrim, R. Glaum, and H. Huppertz, Z. Anorg. Allgem. Chem. **635**, 2002 (2009).

12. J. L. C. Rowsell, N. J. Taylor, and L. F. Nazar, J. Solid State Chem. **174**, 189 (2003).

13. T. Yang, Y. Wang, D. Yang, G. Li, and J. Lin, Solid State Sci. **19**, 32 (2013).

14. G. Kresse and J. Hafner, Phys. Rev. B **47**, 558 (1993).

15. G. Kresse and J. Furthmuller, Phys. Rev. B **54**, 11169 (1996).

16. G. Kresse and D. Joubert, Phys. Rev. B **59**, 1758 (1999).

17. P. E. Blochl, Phys. Rev. B **50**, 17953 (1994).

18. J. P. Perdew, in *Electronic Structures of Solids'91*, Ed. by P. Ziesche and H. Eschrig (Akademie, Berlin, 1991), p. 11.

19. H. J. Monkhorst and J. D. Pack, Phys. Rev. B **13**, 5188 (1976).

20. S. L. Dudarev, G. A. Botton, S. Y. Savrasov, C. J. Humphreys, and A. P. Sutton, Phys. Rev. B **57**, 1505 (1998).

21. K. Momma and F. Izumi, J. Appl. Crystallogr. **44**, 1272 (2011).

22. M. Gajdoš, K. Hummer, G. Kresse, J. Furthmüller, and F. Bechstedt, Phys. Rev. B **73**, 045112 (2006).

Translated by E. Bondareva